

## A model of heat transfer taking place in thermographic test stand

J. Kaczmarczyk <sup>a</sup>, M. Rojek <sup>b</sup>, G. Wróbel <sup>b</sup>, J. Stabik <sup>b,\*</sup>

<sup>a</sup> Division of Applied Mechanics, Silesian University of Technology,  
ul. Konarskiego 18a, 44-100 Gliwice, Poland

<sup>b</sup> Division of Metal and Polymer Materials Processing,  
Institute of Engineering Materials and Biomaterials, Silesian University of Technology,  
ul. Konarskiego 18a, 44-100 Gliwice, Poland

\* Corresponding author: E-mail address: jozef.stabik@polsl.pl

Received 22.01.2008; published in revised form 01.03.2008

### Materials

#### ABSTRACT

**Purpose:** The aim of this paper is to present a model describing heat transfer taking place during thermovision testing of polymer composites. Thermographic tests were undertaken to identify thermal properties of searched material and to correlate them with operational characteristics.

**Design/methodology/approach:** Heat transfer model of thermographic testing stand of our own design was elaborated. The model was applied as a tool of tested material characteristics identification, forming the basis of laminate degradation degree diagnosis.

**Findings:** The most essential result of the project is the physical heat transfer model. Good conformity between model predictions and exemplary experimental results was achieved. The set of physical characteristics describing thermal state of composite was identified and introduced into the model.

**Research limitations/implications:** Experimental results of heat transfer through the composite mounted in thermographic testing stand proved the correctness of developed model. Results of physical properties identification showed the possibility of non-destructive diagnosis of wide class of materials, namely polymeric composites.

**Practical implications:** Results of presented project together with results of planned experimental programme devoted to elaboration of diagnostic relations enable to apply thermography directly to the state of polymeric structural materials assessment. Especially the degree of material degradation may be estimated.

**Originality/value:** Originality of the project is based on possibility of practical application of the model to simulate heat transfer through tested sample mounted in thermographic test stand. Proposed scope of diagnostic tests was not interesting for scientists till now.

**Keywords:** Polymer composite; Thermovision; Diagnostics; Degradation; Heat transfer

### 1. Introduction

In the case of polymer composites undergoing degrading ageing processes, changes of surface appearance can not be used as a measure of the degree of material degradation. Usually surface colour changes occur within thin outer layer and considerably precede any inner degradation processes. When degradation occurs in a dispersive way within the element volume, without any additional visible

external changes of physical and geometrical properties or when surface changes do not correspond to internal degradation processes, a classical visual inspection of a structure may not reveal any dangerous conditions. Therefore, there is a need of searching non-destructive methods of investigation of the degradation degree, which will be able to reveal these dispersive changes. Authors made such an attempt using non-destructive thermography technique with reference to thermally aged polymer composites.

Thermovision is more and more widely used as non-destructive method of materials and among them polymers testing [1-9]. Thermovision diagnosis makes use of time and space characteristics of surface temperature distribution of searched object. The surface temperature values and distribution may be a result of thermal processes taking place in the object in working conditions (passive thermography) or may be a result of thermal activation caused by researcher (active thermography). In the presented project the second case is described where thermal process was activated in composite sample by heating using infrared radiator. The purpose of all diagnosis techniques is to evaluate hazardous changes of different object properties, especially strength and rheological characteristics, due to various degrading processes [10-14]. The main advantage of thermovision testing in described research is its non-destructive nature and possibility of non-destructive estimation of characteristics related with degrading factors taking place in ageing and fatigue processes.

In the present project the following methodology was applied:

- Samples of epoxy-glass composite were subjected to thermal ageing thus causing their degradation;
- Physical model of heat transfer in sample heated and cooled in thermovision testing stand was worked out;
- On the basis of physical model, heat transfer numerical model and computational programme was elaborated;
- Degraded composites were tested using active thermography;
- Experimental results of temperature distribution and its time alternation were compared with numerical predictions.

## 2. Physical model of heat transfer process

The model of heat transfer in composite sample mounted in thermographic testing stand and assumed boundary conditions are schematically shown in Fig. 1. Because of sample symmetry only one half was modelled and is presented. The heat transfer process through test piece is non-stationary. It is the result of continually changing condition of heat exchange during testing and unstable thermal state of test piece in both stages of testing process. Two characteristic phases of thermal process taking place in the test piece and composing the experiment are:

- Thermal activation of test piece by IR heating;
- Cooling down of test piece.

In the described project experimental schedule assumes the following possibilities:

- Thermal activation of test piece in the constant and strictly defined conditions;
- Thermovision registration of surface temperature distribution being the result of activation process;
- Finding the temperature distribution characteristics highly correlated with functional characteristics of tested material;
- Elaboration of empirical diagnostic functions relating temperature distribution characteristics and functional properties of searched materials.

Assumption stated in (b) is related with technical conditions of temperature registration with thermovision camera and also with accessibility of these surfaces of the object that are the most effective, taking into account the purpose of the research programme. Assumption (c) states the possibility of selection,

among infinite number of time-space temperature distribution characteristics possible to determine in given experimental conditions, the one that is correlated with diagnosed material property in a manner enabling formulation of diagnostic function according to the assumption (d). This characteristic will be called in the following text the 'thermographic characteristic'. The basic condition of effectiveness of elaborated method is fulfilment of the assumption (a). It means that experimental conditions must be such that it will be possible to separate changes of material properties analyzed in diagnostic procedure from other factors influencing chosen thermographic characteristic.

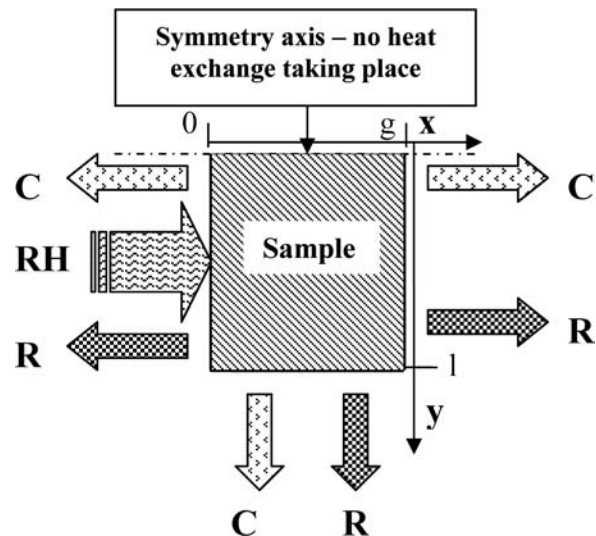


Fig. 1. The modelled half of sample cross section together with boundary conditions; RH – heater radiation flux, C – convection flux, R – sample radiation flux

The beginning of the activation process is determined by initial thermal state of test piece. It is the thermal equilibrium state of the test piece placed in environment. The temperature is the same within all volume of test piece and equal to environment temperature. Together with the test piece exposition to the heater radiation begins the process of heat exchange between the test piece and environment. The dominant form of heat exchange, taking into account great temperature difference between heater and test piece surface, is radiation. Heat exchange process due to radiation is very complicated [15-17]. The reason is that in this process radiator, test piece and environment take part simultaneously. Instantaneous heat flux absorbed by the test piece is the result of thermal balance of the heat flux reaching the surface of the test piece and going from the radiator,  $\Phi_H$  and heat flux resulting from heat exchange between the test piece and environment  $\Phi_E$ :

$$\Phi = \Phi_H + \Phi_E \quad (1)$$

In the local range the similar balance can be written for radiation in chosen point on the surface of the sample, P:

$$E(P) = E_H(P) + E_E(P) \quad (2)$$

Radiation intensity from the point P to environment  $E_E(P)$ , assuming that the specimen surface is black body, according to Stefan – Boltzmann law, was equal:

$$E_E(P) = \varepsilon_1 \cdot \sigma_0 \cdot T^4 \quad (3)$$

where  $\sigma_0 = 5,7 \cdot 10^{-8} \text{ W/m}^2 \text{ K}^4$  is black body radiation constant,  $\varepsilon_1$  is the surface emissivity at the point P and T is the thermodynamic temperature.

Radiation intensity  $E_H(P)$  of energy going from the heater and reaching the point P determines the energy reaching this point relative to area  $dF_P$  around point P. Total energy radiated by heater surface with area, F, (Fig. 2) may be written as:

$$Q = E_R \cdot F \cdot \Psi, \quad (4)$$

where  $E_R$  is radiation intensity of heater surface in temperature,  $T_R$ , and characterized by surface emissivity,  $\varepsilon_2$ ,

$$E_R = \varepsilon_2 \cdot \sigma_0 \cdot T_R^4, \quad (5)$$

The symbol  $\Psi$  in eq.4 denotes the configuration coefficient:

$$\Psi = \frac{1}{F} \iint_{FF_P} \frac{\cos^2 \varphi}{\pi r^2} dF dF_P. \quad (6)$$

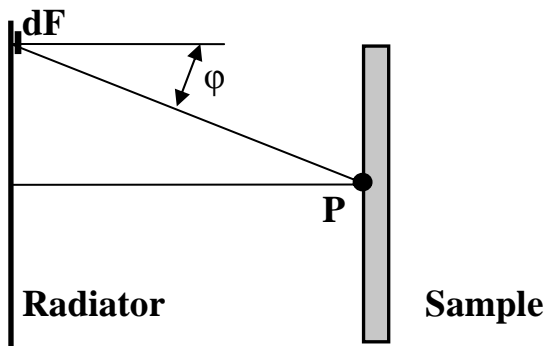


Fig. 2. Schema of heater and test piece arrangement together with symbols used in the text

Radiation intensity  $E_H(P)$  can now be written as

$$E_H(P) = \frac{dQ}{dF_P} = E_R \int_F \frac{\cos^2 \varphi}{\pi r^2} dF, \quad (7a)$$

$$E_H(P) = \varepsilon_2 \cdot \sigma_0 \cdot T_R^4 \int_F \frac{\cos^2 \varphi}{\pi r^2} dF. \quad (7b)$$

Resultant radiation intensity in the surroundings of the point P, taking into account eq.(2) and (7) is equal:

$$E(P) = \varepsilon_1 \varepsilon_2 \sigma_0 (T_R^4 - T^4) \int_F \frac{\cos^2 \varphi}{\pi r^2} dF - \varepsilon_1 \sigma_0 T^4 \quad (8)$$

Assuming that radiation is dominant and the only form of heat exchange at this stage of experiment, we can assume also that radiation with intensity E(P) on test piece surface transforms into heat flux q(P). The temperature of test piece surface, T, changes during activation (heating) process, so also q(P) and E(P) change with time, t:

$$q(P) = q(P, t) = E(P, t) \quad (9)$$

The heat flow within the test piece is circumscribed by Fourier's law:

$$\nabla^T (k \nabla) T + (Q - c_p \cdot \rho \frac{\partial T}{\partial t}) = 0 \quad (10)$$

where: k – anisotropic thermal conductivities matrix, Q – thermal power of heat sources (the rate of heat generation within test piece volume),  $c_p$  – specific heat,  $\rho$  – material density.

Assuming that in the sufficient volume around the point P boundary conditions (9) are homogeneous (heating intensity, q, was the same), we may describe heat transfer in the test piece as unidirectional and proceeding in the direction normal to heated surface. In this case eq. (10) may be simplified to the form:

$$k \frac{\partial^2}{\partial x^2} T + (Q - c_p \cdot \rho \frac{\partial T}{\partial t}) = 0 \quad (11)$$

where x is coordinate describing the depth on the cross section of the test piece perpendicular to heated surface (Fig. 1). When we assume that the heated surface is placed at the origin of the coordinate system ( $x = 0$ ), for the opposite side of the test piece  $x = g$ , where g is the test piece thickness. At the outer surfaces of the sample convective heat exchange with environment take also place. Convection flux density,  $q_k$ , at the sample surface is equal:

$$q_k = \alpha_k (T - T_e), \quad (12)$$

where  $\alpha_k$  is the surface convection heat conductance and  $T_e$  is the environment temperature.

Equation (11) together with boundary conditions (9) and (12) describe the activation stage of the experiment process. We designate the time of the activation as  $\Delta t_1$ . The end of this stage

of experiment is simultaneously the beginning of cooling down stage. For the second stage the boundary condition (9) must be changed. Rewriting eq. (8) for this stage, describing radiation intensity at the point P surroundings, only component defining radiation of test piece surface to environment have to be taken into consideration:

$$q(P, t) = E(P, t) = \varepsilon_1 \cdot \sigma_0 \cdot T(t)^4 \quad (13)$$

Thermal process taking place at this stage is described by eq.(11) together with the boundary conditions (12) and (13) at  $x=0$  and  $x=g$  (Fig. 1).

### 3. Numerical procedure

Numerical calculations were conducted using more and popular these days finite differences method [18,19]. A special computer programme was elaborated and written in object oriented programming language C++. Separate procedures were prepared to simulate both stages of thermal process in the test piece. The programme has a possibility to control the time step by comparing it with the time step calculated using procedure stability criteria. Without this control mechanism there is a possibility that some temperature results fall below absolute zero, what is physically impossible.

Using the above mentioned programme the heat flow at the central cross section of the sample was modelled (Fig. 1). Because of the cross section symmetry only one half of this area (10mmx10mm) was introduced into the programme. Modelled area was divided in every direction into 30 segment thus forming 900 elements. Calculations were performed separately for both thermal stages of the experiment. Boundary conditions assumed for heating stage are shown in Fig. 1. At cooling stage radiation flux emitted by IR heater (RH) was turned off. The rest of boundary conditions were the same as at the heating stage. At the beginning of calculations the following values of density, specific heat and conductivity were assumed (according to literature and producer data):

$$\begin{aligned} \rho &= 1,89 \text{ g/cm}^3; \\ c_p &= 852,9 \text{ J/(kg K)}; \\ k &= 0,575 \text{ W/(m K)}. \end{aligned}$$

Heat flux adsorbed by the sample surface in the modelled region, calculated according to relations given in section 2, was equal  $q = 11,0 \text{ kW/m}^2$ .

Taking into account measured temperature distribution, it was assumed additionally that this heat flux was not evenly distributed on the sample wideness but according to the following distribution function:

$$q = q_0 + q_1 \cdot \frac{l^2 - y^2}{l^2} \quad (14)$$

$$\text{where: } q_0 = -8,8 \frac{\text{kW}}{\text{m}^2}, \quad q_1 = -2,2 \frac{\text{kW}}{\text{m}^2}, \quad l = 10\text{mm},$$

$y$  – coordinate as shown in Fig. 1.

This assumption was also made taking into account differences in sample heating due to distance differences between point P and heater surface element  $dF$  (see Fig. 2).

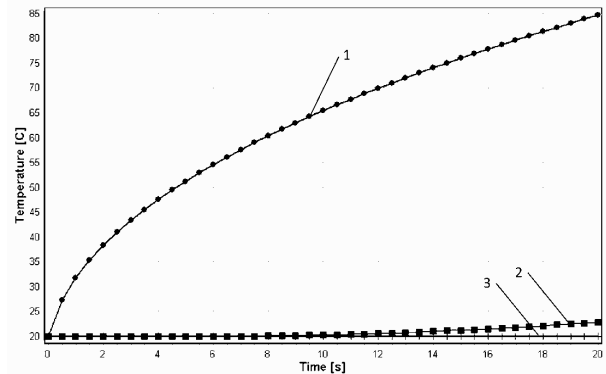


Fig. 3. Dependence of temperature on time at the heating stage of experiment. 1 – point at the heated surface, 2 – point at  $x = 0.5g$ , 3 – point at the surface opposite to the heated one

Elaborated numerical model of heat transfer in the sample allowed to determine the temperature distribution in arbitral point within sample volume and at sample surface. Fig. 3 presents exemplary curves of temperature increase with time for three points, the first one on heated surface, the second one at the centre of sample thickness and the third one on the surface opposite to the heated one.

### 4. Application of the model to degradation process diagnosis

Epoxy-glass laminate (TSE-5, IZO-Erg, Poland) was subjected to thermal ageing. Samples with dimensions 250x20x10mm were aged at three temperatures: 200, 220 and 240°C. Samples were degraded up to 2600 hours. Aged samples were subsequently tested with thermovision camera. Schematic draw presenting thermovision test stand is shown in Fig.4.

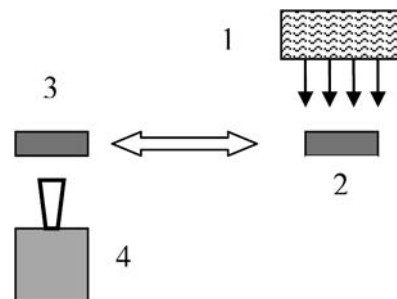


Fig. 4. Thermovision test stand: 1 – IR heater, 2 – the sample in heating position, 3 – the sample in temperature scanning position, 4- thermovision camera

The constructed test stand consists of:

- Clamping device with test piece,
- Heat activator (IR radiator),
- Thermovision camera,
- Auxiliary equipment enabling constant experimental conditions (shields, slides etc.).

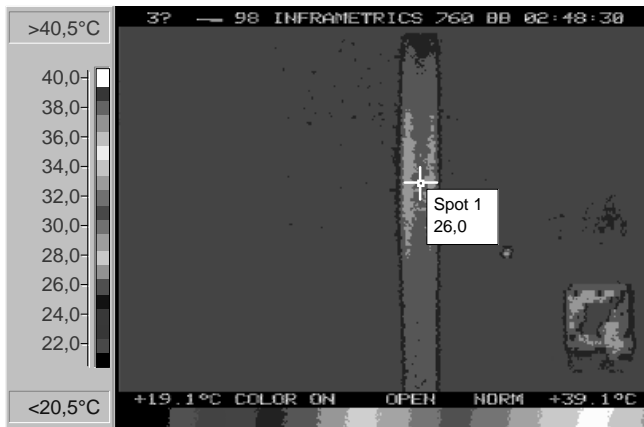


Fig. 5. Thermographic image for sample aged 1992 hours in 200 °C captured 30 seconds after the end of heating

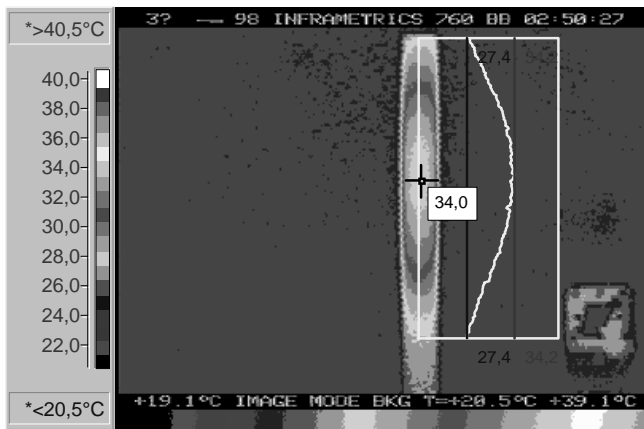


Fig. 6. Thermographic image for sample aged 1992 hours in 200 °C captured 165 seconds after the end of heating

Thermovision camera was used to observe heat flow process activated in sample by IR heater with constant surface temperature. The heater and the sample were mounted vertically at constant distance. The purpose of the project was to define experimental conditions for which searched diagnostic relation was the most explicit. It was assumed that diagnostically effective thermographic characteristic had to be defined for changing in time temperature distribution measured at surface opposite to heated one. This distribution was among others affected by material thermal properties, defined in cross section of sample, which on the other hand are affected by degrading processes

being the result of ageing. The starting moment of temperature distribution evaluation was determined by time of heating and time needed to rearrange testing stand from heating to temperature scanning position. Examples of thermovision images registered 30 and 165 seconds after the end of heating for samples aged 1992 hours at 200 °C are shown in Fig. 5 and Fig. 6. Thermovision images registered 60 and 153 seconds after the end of heating for samples aged 1992 hours in higher temperature, 240 °C, are shown in Fig. 7 and Fig. 8.

The images were taken every three seconds and registered by computer being a part of thermovision camera equipment. A special software in this computer enabled temperature distribution evaluation. For the purpose of described research the temperatures at the central point of the sample was the most important. These temperatures allowed to plot curves describing temperature increase at this point with time. Examples of such curves are presented in Fig. 9 and 10 for two temperatures of ageing: 200 °C and 240 °C. Lower temperatures registered for samples aged at 240 °C are clearly visibly.

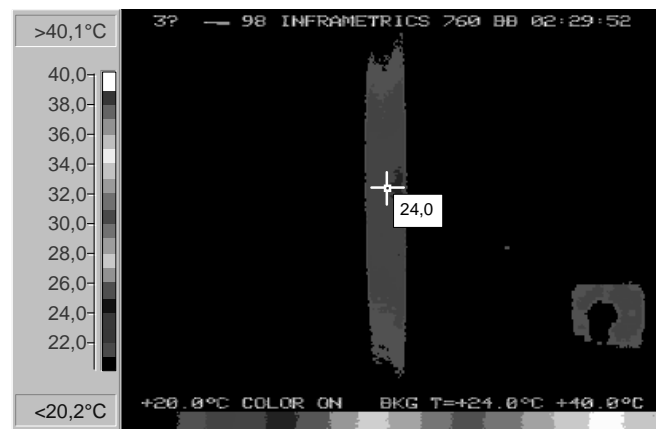


Fig. 7. Thermographic image for sample aged 1992 hours in 240 °C captured 60 seconds after the end of heating

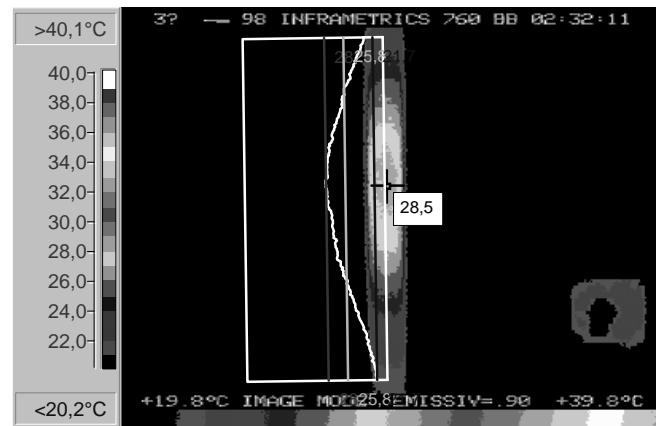


Fig. 8. Thermographic image for sample aged 1992 hours in 240 °C captured 153 seconds after the end of heating

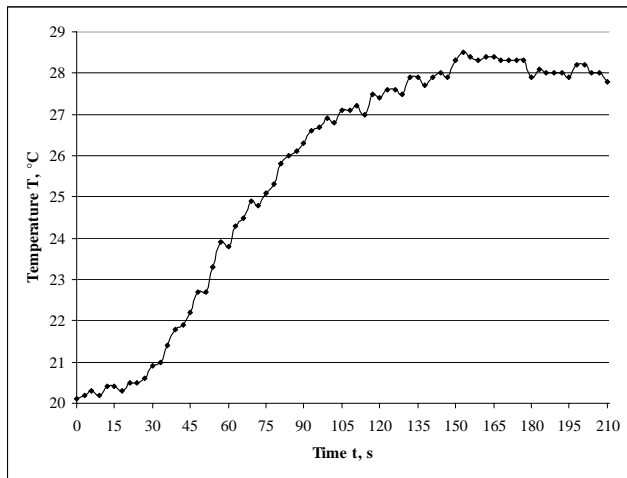


Fig. 9. Temperature – time dependence for central point of the sample aged 1992 hours in 200 °C

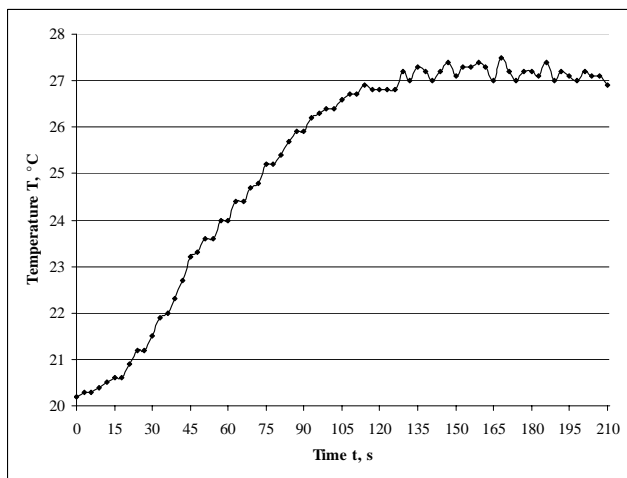


Fig. 10. Temperature – time dependence for central point of the sample aged 1992 hours in 240 °C

In presented methodology very important was experimental conditions constancy and repeatability. This repeatability of conditions refers mainly to:

- Heater surface temperature;
- Heater position;
- Time of radiation;
- Moment of the beginning of temperature registration;
- Geometry and physical properties of samples and their surface (roughness, thermal emissivity);
- Position and measuring range of thermovision camera;
- Test stand environment.

Fulfilment of above mentioned repeatability conditions allows to expect that differences in thermal processes registered by

thermovision camera were the result mainly of the changes of thermal properties of tested sample material. If these changes were the result of structural degradation of tested polymer or composite then the hypothesis that thermographic characteristics are correlated with material characteristics seems to be justifiable. Conditions of samples testing were in accordance with section 2. Constant heating time (20 seconds) was applied for all samples. Samples were heated with infrared radiator (Elstein HTS/2) with 500W thermal power. Thermovisionic images were registered using Inframetrics 760 camera. On the basis of thermographic images the temperature of central point of the surface opposite to heated one was determined. All experimental parameters together with material data, test stand characteristics and geometry were introduced into the physical heat transfer model described in section 2. The same data were introduced to numerical model presented in section 3. Afterwards numerical simulation of heat transfer through the sample was performed.

Presented model was applied to evaluate the influence of structural changes caused by degradation on chosen diagnostic thermographic characteristics [20-22]. Decrease of main strength characteristics, static, dynamic and fatigue, is the most pronounced manifestation of degrading processes advancement. Results of mentioned degrading processes are of microscopic scale and are dispersed in whole volume of the object. Structural changes take place in polymeric matrix and in interface between polymer matrix. They bring to micro-cracks formation and propagation. Micro-cracks facilitates aggressive media penetration and further accelerate degradation. Finally reinforcing particles (fibres) can be damaged. All these imperfections and discontinuities are supposed to influence thermal properties of composite. Especially thermal conductivity and specific heat of the composite are expected to be influenced by matrix degradation, micro-cracks, adhesion loss and other discontinuities.

Research project assumed possibility of determination in described conditions the thermographic characteristic highly correlated with diagnosed material characteristics. The range of possible solutions is very wide. It is determined by all experimental conditions and also by type and parameters of searched characteristic. It confirms the necessity of searching described effective thermographic characteristic with the help of numerical model simulating heat transfer process in case of presented testing stand.

Described heat transfer model for test stand was verified for composite comparing numerical values with those achieved using thermography. After that changes of thermographic characteristics were simulated in numerical model by variation of mean values of composite thermal properties.

Fig. 11 presents dependence of temperature at the central point of heated surface of the sample aged 1992 hours at temperature 200°C. The singular point of the curve represents the moment of the end of heating and the beginning of cooling down.

Measured and numerically calculated temperatures at the central point of the surface opposite to heated one for the same sample are shown in Fig.12. First 230 seconds of the second stage of experiment are presented.

Analogous simulations and calculations were performed for sample aged the same time but at 240°C. Results of calculations and thermovision temperature measurements are presented in Fig. 13 and Fig. 14.

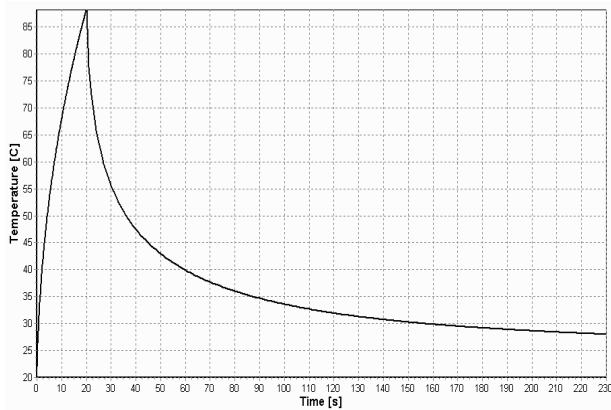


Fig. 11. The dependence of temperature on time at central point of heated surface of the sample aged 1992 hours at temperature 200°C

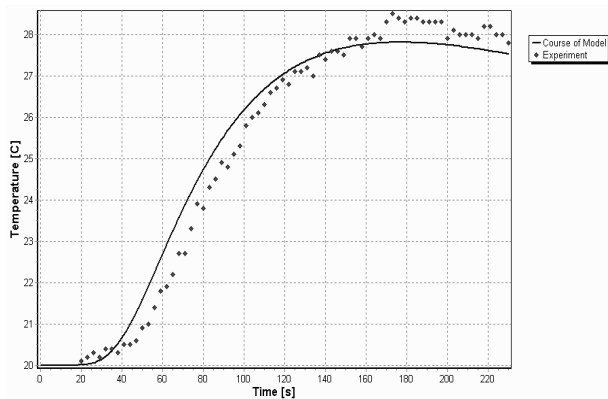


Fig. 12. Comparison of calculated (solid line) and measured (dots) temperatures at the central point of the surface opposite to heated one of the sample aged 1992 hours at temperature 200°C

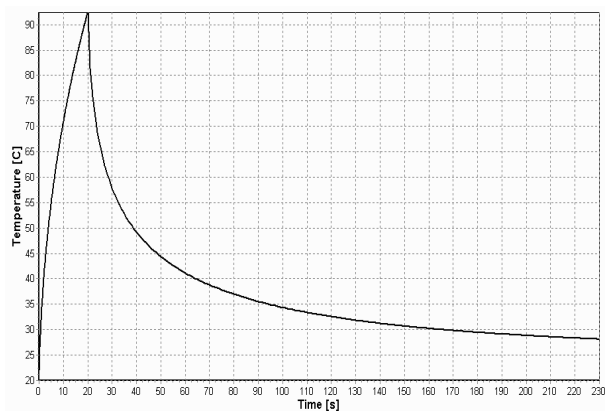


Fig. 13. The dependence of temperature on time at central point of heated surface of the sample aged 1992 hours at temperature 240°C

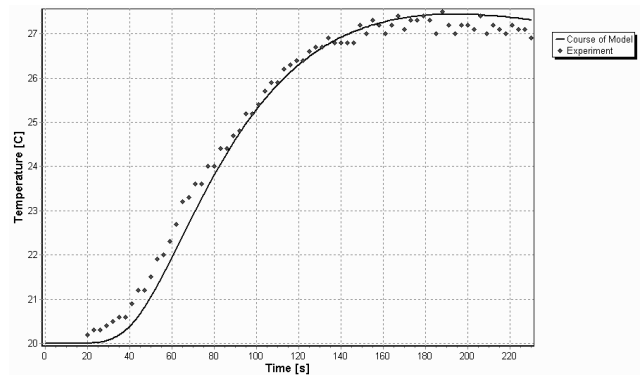


Fig. 14. Comparison of calculated (solid line) and measured (dots) temperatures at the central point of the surface opposite to heated one of the sample aged 1992 hours at temperature 240°C

The following features of achieved dependences were analyzed: the moment of the beginning of temperature increase, the rate of temperature increase at the initial period and the maximum value of temperature. The conformity of numerical with experimental results was achieved by selection of physical characteristics of material such as thermal conductivity,  $k$ , specific heat,  $c_p$ , and surface emissivity,  $\varepsilon_1$ . Results presented in Fig. 11 to 14 were calculated for typical epoxy-glass thermal characteristics values (according to literature and producer's data):

$$c_p = 852,9 \text{ J/(kg K)},$$

$$\varepsilon_1 = 0,8.$$

The main result of thermal ageing was the thermal conductivity coefficient change. For non-aged samples the best accordance between calculated and measured temperatures was achieved when thermal conductivity coefficient was taken as  $k = 0,35 \text{ W/(m K)}$ . For samples aged at 200°C the best results were achieved when  $k = 0,31 \text{ W/(m K)}$  and analogous value for sample aged at 240°C was  $k = 0,27 \text{ W/(m K)}$ . The results clearly showed that the higher is temperature of ageing (the greater degree of degradation) the lower is thermal conductivity of epoxy-glass composite. It is in accordance with what was expected because thermal ageing is one of processes resulting in dispersed micro-defects formation in composite volume. These defects increase thermal resistance of the composite what is manifested by thermal conductivity coefficient increase.

## 5. Conclusions

1. Elaborated physical and numerical model of heat transfer in the sample, subjected to active thermovision testing, allowed to determine the temperature distribution in arbitrary point within sample volume and at sample surface.
2. Results of numerical simulation and results achieved using thermovision camera were in good conformity.
3. The results showed that the higher was temperature of ageing the lower was thermal conductivity of epoxy-glass composite.

4. Worked out methods and algorithms of numerical simulation allowed diagnosis of thermal degradation degree of polymer composite.
5. The thermovision non-destructive evaluation of thermal properties of structural materials can be applied as a method of determination of strength and other properties deterioration.

## Acknowledgements

This work was financially supported by Polish Minister of Science and Higher Education as a part of project N501 029 32/2474.

## References

- [1] P.V. Xavier Maldague, Theory and Practice of Infrared Technology for Nondestructive Testing, John Wiley, Interscience, New York, 2001.
- [2] S. Poloszyk, Active thermovision in non-destructive testing, Proceedings of the Conference Manufacturing'01, Poznań 2001, 221-228 (in Polish).
- [3] D. Bates, G. Smith, D. Lu, J. Hewitt, Rapid thermal non destructive testing of aircraft components, Composites B31 (2001) 75-185.
- [4] N. Rajic, Principal component thermography for flaw contrast enhancement and flaw depth characterization in composites structures, Composite Structures 58 (2002) 521-528.
- [5] C. Meola, G. M. Carlomagno, A. Squillace, A. Vitiello, Non-destructive evaluation of aerospace materials with lock-in thermography, Engineering Failure Analysis 13 (2006) 380-388.
- [6] E.G. Hanneke, K.L. Reifsnider, W.W. Stinchcomb, Thermography - An NDI Method for Damage Detection, Journal of Metals 31 (1979) 11-15.
- [7] G. Muzia, Z. Rdzawski, M. Rojek, J. Stabik, G. Wróbel, Diagnostics basis of thermographic investigation of epoxy-glass composites' degradation process, Proceedings of the International Conference "Machine Building and Technology of XXI Century", Donieck, 2007, 167-170.
- [8] G. Muzia, Z. Rdzawski, M. Rojek, J. Stabik, G. Wróbel, Diagnostic basis of thermographic investigation of epoxy-glass composites' degradation process, Journal of Achievements in Materials and Manufacturing Engineering 24/2 (2007) 123-126.
- [9] G. Wróbel, G. Muzia, Z. Rdzawski, M. Rojek, J. Stabik, Thermographic diagnosis of fatigue degradation of epoxy-glass composites, Journal of Achievements in Materials and Manufacturing Engineering 24/1 (2007) 131-136.
- [10] I.M. Daniel, T. Liber, Non-destructive Evaluation Techniques for Composite materials, Proceedings of 12<sup>th</sup> Symposium on NDE, ASNT and NTIAC, San Antonio, TX, 1979, 226-244.
- [11] J. Deputat, Non destructive testing of materials properties, Gamma Publisher, Warsaw, 1997.
- [12] P.K. Mallick, Nondestructive tests. Composites Engineering Handbook, New York, Basel, Hong Kong, 1997.
- [13] M. Rojek, J. Stabik, S. Sokół, Fatigue and ultrasonic testing of epoxy-glass composites, Journal of Achievements in Materials and Manufacturing Engineering 20 (2007) 183-186.
- [14] G. Wróbel, Ł. Wierzbicki, Ultrasonic methods in diagnostics of glass polyester composites, Journal of Achievements in Materials and Manufacturing Engineering 20 (2007) 206-206.
- [15] F. Kreith, Principles of heat transfer, IEP – A Dun-Donnelley Publisher, New York, 1976.
- [16] S. Ochęduszek, Applied thermodynamics, WNT, Warsaw 1970 (in Polish).
- [17] E.H. Wichmann, Quantum Physics, PWN, Warsaw 1973 (in Polish).
- [18] J. Szmelter, Computational methods in mechanics, National Scientific Publishing House (PWN), Warsaw 1980 (in Polish).
- [19] E. Majchrzak, B. Mochnacki, Numerical Methods, Publishing House of Silesian University in Gliwice, 2004 (in Polish).
- [20] N. Grassie, G. Scott Polymer degradation and stabilisation, Cambridge University Press, 1985.
- [21] A. Balin, G. Junak, Investigation of cyclic creep of surgical cements, Archives of Materials Science and Engineering 28/4 (2007) 281-284.
- [22] A. Balin, G. Junak, Low-cycle fatigue of surgical cements, Journal of Achievements in Materials and Manufacturing Engineering 20 (2007) 211-214.